Laser Additive Manufacturing Principle and Technology of Biomaterials

生物材料的激光增材制造原理与技术

Cijun Shuai, Shuping Peng,
Ping Wu, Pei Feng.

西安交通大学出版社
XI'AN JIAOTONG UNIVERSITY PRESS

Laser Additive Manufacturing Principle and Technology of Biomaterials

生物材料的激光增材制造原理与技术

Cijun Shuai, Shuping Peng,
Ping Wu, Pei Feng. 著

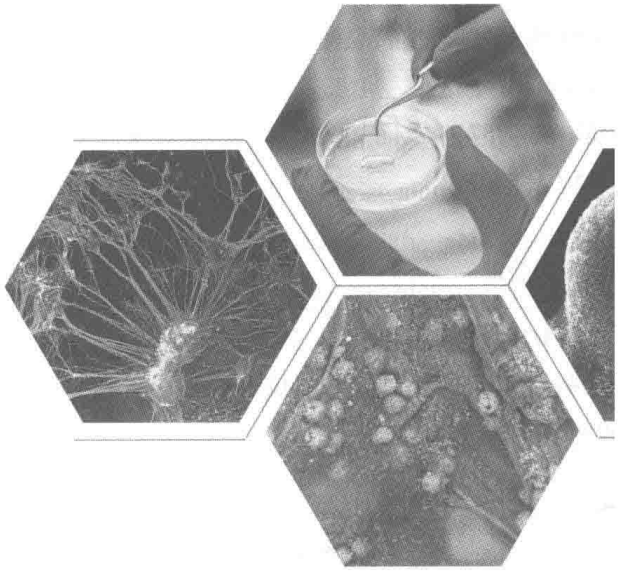

西安交通大学出版社
XI'AN JIAOTONG UNIVERSITY PRESS

图书在版编目（CIP）数据

生物材料的激光增材制造原理与技术 = Laser Additive Manufacturing Principle and Technology of Biomaterials : 英文 / 帅词俊等著 . —西安：西安交通大学出版社，2016. 12

ISBN 978-7-5605-9343-2

Ⅰ . ①生… Ⅱ . ①帅… Ⅲ . ①生物材料—激光技术 Ⅳ . ① R318.08

中国版本图书馆 CIP 数据核字（2017）第 000404 号

书　　名　Laser Additive Manufacturing Principle and Technology of Biomaterials
　　生物材料的激光增材制造原理与技术

著　　者　帅词俊　彭淑平　吴　萍　冯　佩

责任编辑　魏　杰　贺彦峰

出版发行　西安交通大学出版社
　　（西安市兴庆南路 10 号　邮政编码 710049）

网　　址　http://www.xjtupress.com

电　　话　（029）82668357　82667874（发行中心）
　　（029）82668315（总编办）

传　　真　（029）82668280

印　　刷　长沙市宏发印刷有限公司

开　　本　787mm × 1092mm　1/16　　印张　20.5　　字数　429 千字

版次印次　2017 年 1 月第 1 版　2017 年 1 月第 1 次印刷

书　　号　ISBN 978-7-5605-9343-2

定　　价　128.00 元

读者购书、书店添货、如发现印装质量问题，请与本社发行中心联系、调换。

Forward

Tissue repair and regeneration have become a worldwide problem of human's infinite pursuit and continuous exploration. And the demands for biomaterial are growing with the increase of accidental trauma and aging population. The market scale of the global biomaterials increases by above 10 percent a year since 2010. The market growth rate of the biomaterial industry is reaching to 28% in our country. According to conservative estimates, the sales will reach 120 billion dollar by 2020. However, both the research and development ability of biomaterials are weak in our country. Moreover, the technical level of biological products is still at the primary stage and industrialization of research findings is difficult. The high-end biomaterials are mainly dependent on import at present. The huge pressure of healthcare needs to more than one billion people and weak foundation of biomaterials has become a sharp controversy.

At present, the biomaterial sconsist of bioceramics, biopolymer and biometal. Bioceramics are deemed as a kind of the most potential bone repair material because of their good biocompatibility, biodegradation and osteoconduction. But the high brittleness, low toughness and strength of the bioceramics lead to their poor use reliability and damage resistance. Biopolymer is one of the most extensively studied biomaterials owing to the favorable biocompatibility, biodegradation and good processing formation performance. But there exist many disadvantages of biopolymer, such as poor cellular affinity, low mechanical strength, acid degradation products and easy to cause inflammation, etc. Biometal possesses high mechanical strength, high fatigue resistance and good machinability which have great potential in weight-bearing bone repair. Whereas there are some disadvantages of biometal such as poor biomechanical compatibility, easy to produce harmful metal ions and so on.

In order to repair the defected tissue, biomaterials not only need to have good biological properties andenough mechanical strength, but also should have the consistent shape with the defected area and interconnection of porous structure. But the individual customization of porous biomaterials is facing great challenge in manufacturing by

traditional machining. Laser additive manufacturing technology is an advanced manufacturing technology collecting laser, computer software, materials, machinery, control and other multi-disciplinary knowledge in the integration. It can rapidly print the shape and structure of the required parts according to the three-dimensional computer-aided design (CAD) mode. It can precisely fabricate the parts with any complex structures by using this technique, and can realize the integrated manufacturing of material microstructure and space geometric configuration.

To solve the present problems of biomaterials fabricated by conventional techniques such as poor biomechanics properties, having difficulty in shaping porous structure, poor ability of inducing tissue regeneration, the book proposed the solution that employing laser additive manufacturing technology to form high performance materials with hierarchical pores. Furthermore, a series of key technologies are proposed including forming micro-nano grain by laser rapid solidification, strengthening and toughening by the second phase, making multilevel pore structure, controlling shape and performance simultaneously, etc. The selected 20 refereed papers are grouped under the following four parts:

I. Bioceramic;

II. Bioglass;

III. Biopolymer;

IV. Magnesium alloy.

The work is supported by the (1) The Natural Science Foundation of China (51575537, 81572577); (2) Overseas, Hong Kong & Macao Scholars Collaborated Researching Fund of National Natural Science Foundation of China (81428018); (3) Hunan Provincial Natural Science Foundation of China (14JJ1006, 2016JJ1027); (4) The Project of Innovation-driven Plan of Central South University (2015CXS008, 2016CX023); (5) The fund of the State Key Laboratory of Solidification Processing in NWPU (SKLSP201605); (6) The fund of the State Key Laboratory for Powder Metallurgy.

The author, whose scientific research achievements have been summarized in the book, has long been engaged in the teaching, scientific research, and industrial popularization and application of laseradditive manufacturing technology of biomaterials. In the process of systematic induction, collation and compilation of many years'

research achievements, a large number of papers and treatises of experts and scholars have been consulted and quoted. Furthermore, the great support of the Central South University has been gained. In particular, the heartfelt thanks are expressed to the vast majority of teachers and students for the support and assistance of the publication of the book.

Due to the author's limited knowledge and the rapid development of technology, there are inevitably some shortcomings and mistakes in the book. The author would greatly appreciate receiving criticism and correction from readers.

CONTENTS

Part Ⅰ Bioceramic

A novel $MgO-CaO-SiO_2$ system for fabricating bone scaffolds with improved overall performance*

Abstract: Although forsterite (Mg_2SiO_4) possesses good biocompatibility and suitable mechanical properties, the insufficient bioactivity and degradability hinders its further application. In this study, a novel $MgO-CaO-SiO_2$ system was developed by adding wollastonite ($CaSiO_3$) into Mg_2SiO_4 to fabricate bone scaffolds via selective laser sintering (SLS). The apatite-forming ability and degradability of the scaffolds were enhanced because the degradation of $CaSiO_3$ could form silanol groups, which could offer nucleation sites for apatite. Meanwhile, the mechanical properties of the scaffolds grew with increasing $CaSiO_3$ to 20 wt%. It was explained that the liquid phase of $CaSiO_3$ promoted the densification during sintering due to its low melting point. With the further increase in $CaSiO_3$, the mechanical properties decreased due to the formation of the continuous filling phase. Furthermore, the scaffolds possessed a well-interconnected porous structure and exhibited an ability to support cell adhesion and proliferation.

Key words: $MgO-CaO-SiO_2$ system, forsterite, wollastonite, scaffold, overall performance

1 Introduction

For bone scaffolds, the excellent bioactivity, controlled degradability, osteo-conductive and appropriate mechanical properties were indispensable in meeting clinical requirements[1-4]. Forsterite (Mg_2SiO_4), the $MgO-SiO_2$ system bioceramic, possessed good cytocompatibility and suitable mechanical properties[5,6]. Magnesium, as an important mineral element in bone tissues, played a key role in bone remodeling and skeletal development[7,8]. Silicon, as an indispensable element in human nutrition, was

---

* Hang Sun, Shiwei He, Ping Wu, Chengde Gao, Pei Feng, Tao Xiao, Youwen Deng, Cijun Shuai. A novel $MgO-CaO-SiO_2$ system for fabricating bone scaffolds with improved overall performance. Materials, 2016, 9(4): 287.

associated with improving bone calcification[9,10], while the low degradability and poor bioactivity hindered its further application in bone repair[11].

Wollastonite ($CaSiO_3$), the CaO-SiO_2 system bioceramic, was a representative bioactive material for tissue regeneration due to its strong ability to induce bone-like apatite formation and a fast degradation rate[12-14]. Moreover, it could be used as a reinforcement phase to fill ceramics for further densification[15,16]. Sainz et al. developed $CaSiO_3$-$CaMg(SiO_3)_2$ eutectic bioceramics to be used as bioactive implant materials, and found that they showed high reactivity and proper degradability in simulated body fluid (SBF)[17]. Chang et al. developed hydroxyapatite/wollastonite composite bioceramic for hard tissue repair, suggesting that the introduction of $CaSiO_3$ into hydroxyapatite was an effective method to obtain composites with enhanced mechanical properties, proper dissolution rate and improved bioactivity[18].

In this study, $CaSiO_3$ was incorporated into Mg_2SiO_4 to develop a novel MgO-CaO-SiO_2 system for fabricating bone scaffolds via selective laser sintering (SLS). The apatite-formation ability, degradability, mechanical properties and the MG63 cell responses to scaffolds were investigated.

2 Materials and methods

2.1 Scaffold fabrication

Mg_2SiO_4, which was provided by Alfa Aesar China Co., Ltd. (Tianjin, China), was medical grade material with an average particle size of about 5 μm. $CaSiO_3$, which was provided by Kunshan Huaqiao New Materials Co., Ltd. (Kunshan, China), had a diameter of 0.2 ~ 2 μm. The Mg_2SiO_4 and $CaSiO_3$ powders were mixed in different proportions using the ultrasonic method and the ball mill method. In detail, the Mg_2SiO_4 and $CaSiO_3$ powders were first dispersed in ethanol for 30 min of ultrasonication, and then followed by 30 min of ball mill grinding at room temperature using a variable frequency planet-type grinding mill. Three different-diameter ZrO_2 balls (3, 5 and 10 mm) were mixed as the milling media to enhance the homogeneity. After milling, the obtained powders were dried in a draught drying cabinet at 70 ℃ for 12 h.

The prepared mixed powders were used as sintering raw materials for fabricating the porous scaffolds via SLS. The SLS system contained a laser with an optical focusing system, sintering platform, three-dimensional motion platform and the control system[19]. In the SLS process, the mixed powders were selectively sintered layer by layer to form the interconnected porous scaffold. The relevant process parameters were kept constant as

follows: laser power of 8.5 W; spot diameter of 1 mm; scanning rate of 100 mm/min; scanning line interval of 3.5 mm; and average layer thickness of 0.1 mm.

2.2 Scaffold characterization

The microtopography of the scaffolds was studied by scanning electron microscopy (SEM) (TESCAN MIRA3 LMU, Co., Brno, Czech Republic) completed with energy dispersive spectroscopy (EDS). Before SEM observation, the scaffolds were treated by desiccation and spray platinum (JFC - 1600, JEOL Co., Tokyo, Japan). The phase composition of the scaffolds were determined by X-ray diffraction (XRD) (Rigaku Co., Tokyo, Japan) using a Cu-Kα source (λ = 1.5418 Å) in a range of 10° to 80° with 8°/min scanning rate.

The compression strength of the scaffolds was measured using a microcomputer-controlled electron universal testing machine (WD-D1, Shanghai Zhuoji Instruments Co., Ltd., Shanghai, China). The compression load was applied on scaffolds at a speed of 0.5 mm/min until the scaffolds were completely crushed. The compression strength was calculated by dividing the peak load by the cross-sectional area of the scaffolds. The fracture toughness of the scaffolds was measured using a digital microhardness tester (Shanghai Taming Optical Instrument Co., Shanghai, China). A load of 4.98 N was applied on polished surface for 10 s by a pyramid-shaped diamond indenter to induce indentations and cracks. Then the load and the crack length were used to calculate the fracture toughness (K_{IC}) based on the following Equation (1)[20]:

$$K_{IC} = 0.0824P \times C^{-3/2} \quad (1)$$

where P is the load applied by the indenter and C is the half-length of diagonal crack.

2.3 Degradation behavior

The degradability of the scaffolds was evaluated based on their weight loss in phosphate buffer saline(PBS) solution (pH = 7.4). The scaffolds were soaked in the solution for different periods (7, 14, 21, and 28 days) in an incubator at 37 ℃ and the solution was renewed every 24 h. After the predetermined soaking time, the scaffolds were taken out from the solution, carefully rinsed in ethanol and then desiccated at 70 ℃ for 10 h. The weight of the scaffolds was accurately measured before and after soaking.

2.4 Bioactivity

Bioactivity of the scaffoldswas assessed by detecting the formation of bone-like apatite after soaking in simulated body fluid (SBF). The SBF solution had a similar

composition and concentrations to that of human blood plasma (Table 1)[21]. The scaffolds were soaked in SBF for 14 days in an incubator with a constant temperature of 37 ℃ and the SBF solutions were replaced every other day. After soaking, the scaffolds were carefully rinsed in ethanol and then desiccated at room temperature for further characterization. The morphology and chemical group of bone-like apatite formed on the scaffolds were characterized by SEM and Fourier transform infrared spectroscopy (FTIR) (Thermo Electron Scientific Instruments, Madison, WI, USA), respectively.

Table 1 Ion concentration in SBF and human blood plasma

Ion Type	Ion Concentration/(mmol/L)						
	Na^+	K^+	Mg^{2+}	Ca^{2+}	Cl^-	HCO_3^-	HPO_4^{2-}
Blood Plasma	142.0	5.0	1.5	2.5	103.0	17.0	1.0
SBF	142.0	5.0	1.5	2.5	148.8	4.2	1.0

2.5 Cell culture

Cytocompatibility of the scaffolds was assessed by MG63 osteoblast-like cell (Cellular Biology Institute, Shanghai, China) culture studies in 12-well culture plate. Prior to the cell culture, the scaffolds were immersed in ethyl alcohol solution for 2 h of sterilization, then exposed to ultraviolet light for 15 min and washed with PBS. After that, they were seeded with MG63 cell (20000 cells/well) and cultured in Dulbecco's Modified Eagle's Medium (DMEM) with 10% (v/v) fetal bovine serum at 37 ℃ in a 5% CO_2 humid incubator with the culture media refreshed every three days. After different culture times (three days, five days), the scaffolds were removed from the culture plate and rinsed with PBS to remove the unattached cells. Then, the adherent cells on the scaffolds were fixed with 4% glutaraldehyde (for 30 min) and successively dehydrated in ethanol (70.0%, 80.0%, 90.0% and 100.0%). Afterwards, the scaffolds were dried and sputter-coated with platinum. Finally, the cell-scaffold interactions and cell behavior were visualized using SEM.

Moreover, the cell-scaffolds interaction was also investigated using fluorescence technique. After different culture times, scaffolds were taken out from the culture plate and cleaned with PBS, then settled with buffered ice-cold paraformaldehyde and permeabilized with 0.1% Tween 20. Afterwards, the cells were rinsed again with PBS and preincubated by 1% gelatin in PBS. Subsequently, the cells were incubated for 30 min in the compound of 4 μm EthD-1 and 2 μm calcein AM in PBS. Finally,

Fluorescence microscopies of the cells were visualized using confocal microscope.

2.6 Statistical analysis

All thedata were statistically analyzed using one-way analysis of variance (ANOVA) and shown as mean ± standard deviation ($N = 5$) where appropriate. The level of statistically significance was set at p-value less than 0.05.

3 Results and discussion

3.1 Mixed powders

The Mg_2SiO_4 and $CaSiO_3$ powders were irregular bulk and approximate sphere, respectively (Figure 1a, b). The small $CaSiO_3$ particles (0.2 ~ 2 μm) were randomly distributed on and between the Mg_2SiO_4 particles (about 5 μm) after mixing (Figure 1c). It might benefit the sintering process due to the large specific surface area of $CaSiO_3$. The X-ray diffraction (XRD) patterns of the received Mg_2SiO_4 and $CaSiO_3$ powders (Figure 1d) were consistent with JCPDS (Joint Committee on Powder Diffraction Standards) cards for Mg_2SiO_4 and β-$CaSiO_3$ (JCPDS cards No. 34 – 0189 and No. 84 – 0654) without the peaks of other phases detected.

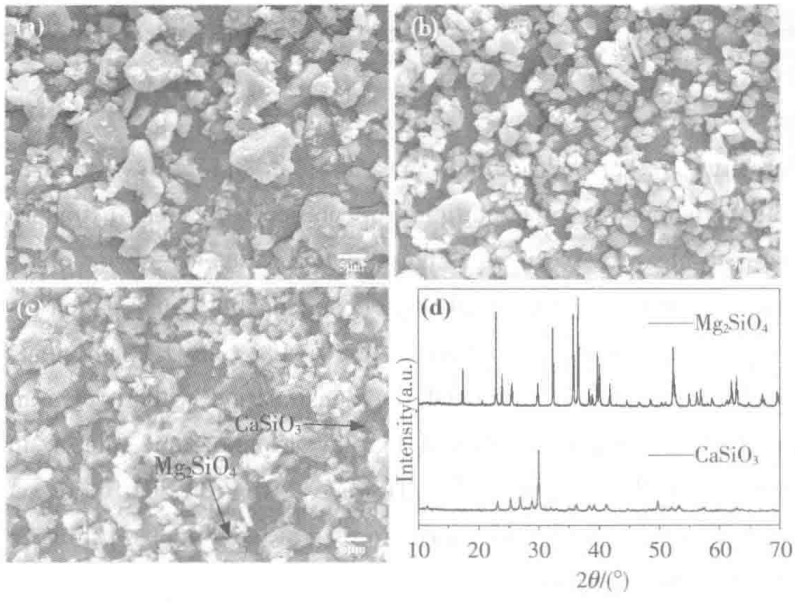

Figure 1 The microstructure of powders: (a) initial forsterite (Mg_2SiO_4); (b) initial wollastonite ($CaSiO_3$); (c) mixed powders; and (d) X-ray diffraction (XRD) patterns

3.2 Scaffolds

The fracture toughness and compression strength of the scaffolds increased with increasing $CaSiO_3$ from 0 to 20 wt%, but began to decrease with further increasing $CaSiO_3$ (Figure 2). In this study, when 20 wt% $CaSiO_3$ was introduced, the scaffolds obtained an optimal fracture toughness and compressive strength of 2.48 ± 0.05 MPa · $m^{1/2}$ and 40.29 ± 1.32 MPa, which represented an improvement of 31.7% and 34.90% compared to the scaffolds without $CaSiO_3$, respectively. It indicated that the mechanical properties of the scaffolds could be effectively strengthened by incorporating $CaSiO_3$.

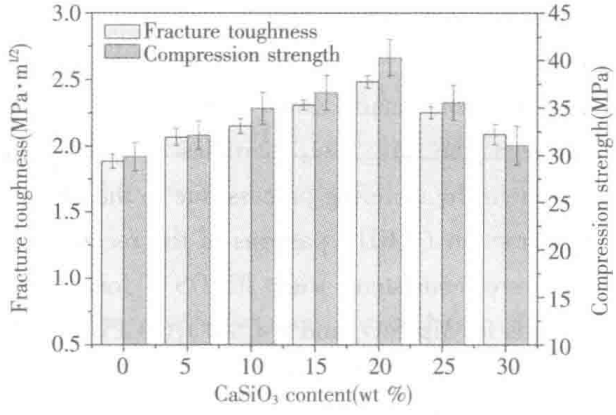

Figure 2 Fracture toughness and compression strength of the scaffolds with different $CaSiO_3$ content

The microstructures of the scaffolds are shown in Figure 3. The scaffolds without $CaSiO_3$ exhibited distinct Mg_2SiO_4 particle appearance with clear boundaries and some clearances between Mg_2SiO_4 particles (Figure 3a). In the case of scaffolds with 10 wt% $CaSiO_3$, a small amount of liquid phase enhanced the densification by filling the clearances (Figure 3b). For the scaffolds with 20 wt% $CaSiO_3$, sufficient liquid phase was formed, which remarkably improved the densification without clearances (Figure 3c, e). The liquid phase was believed to play an important role in improving the mechanical strength of the scaffolds[15,16]. However, when $CaSiO_3$ increased to 25 wt% (Figure 3d), the excessive liquid phase formed a continuous filling phase, which resulted in the decline of mechanical properties.

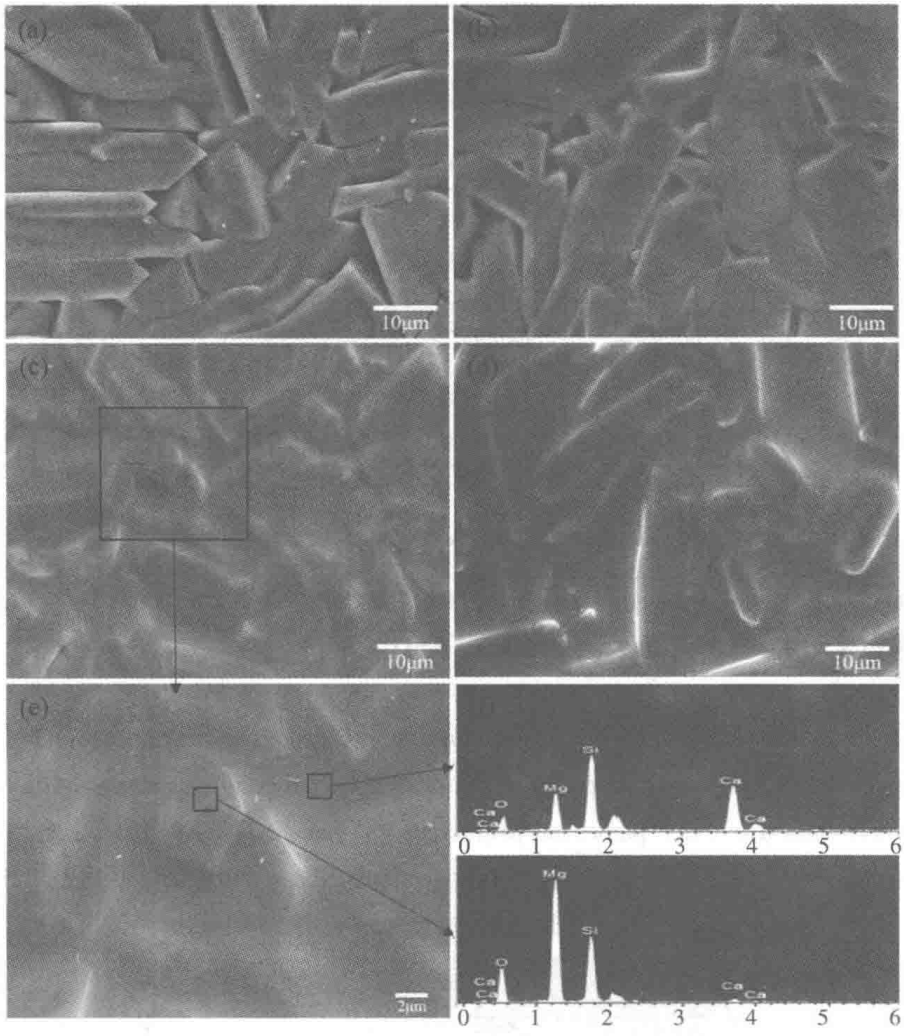

Figure 3 Morphologies of the scaffolds with different $CaSiO_3$ content: (a) 0 wt%; (b) 10 wt%; (c, e) 20 wt%; (d) 25 wt%; and (f, g) energy dispersive spectroscopy spectrums of the scaffold with 20 wt% $CaSiO_3$

The majordiffraction peaks of the scaffolds were consistent with Mg_2SiO_4 (JCPDS card NO. 34 – 0189) (Figure 4), which meant that the scaffolds were mainly composed of Mg_2SiO_4. For the scaffolds with 10, 20, and 25 wt% $CaSiO_3$, some peaks of β-$CaSiO_3$ (JCPDS card No. 84 – 0654) at 2θ = 11.48°, 25.20°, 28.80°, and 30.00° were detected, and gradually increased in intensity with the increase of $CaSiO_3$ (Figure 4b – d). Meanwhile, no distinct peaks of other phase were detected.

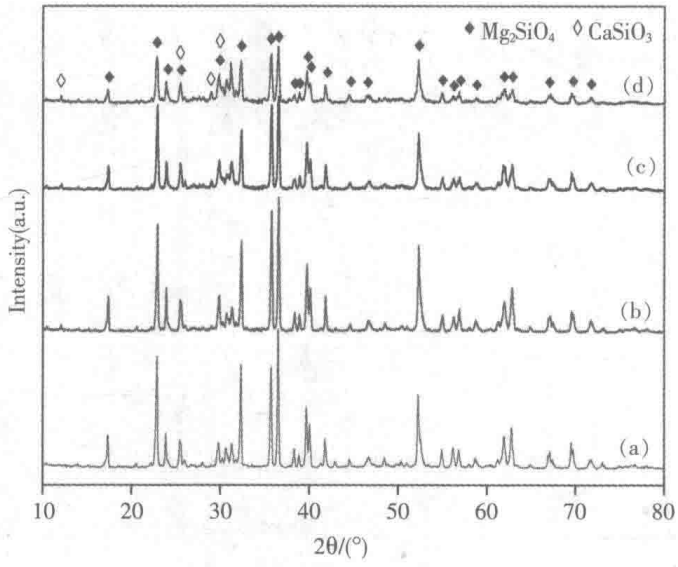

Figure 4 X-ray diffraction patterns of the scaffolds with: (a) 0 wt%; (b) 10 wt%; (c) 20 wt%; and (d) 25 wt% $CaSiO_3$

A scaffold with 20 wt% $CaSiO_3$ was fabricated with geometric dimensions of 14.5 mm × 14.5 mm × 6.5 mm (Figure 5). It possessed an interconnected porous structure with a pore size of about 500 ~ 800 μm. Such porous microstructure was beneficial for cell ingrowth, nutrients transport and waste products excreted from the scaffold. These demonstrated that SLS have a good ability to fabricate interconnected porous structure of the scaffolds.

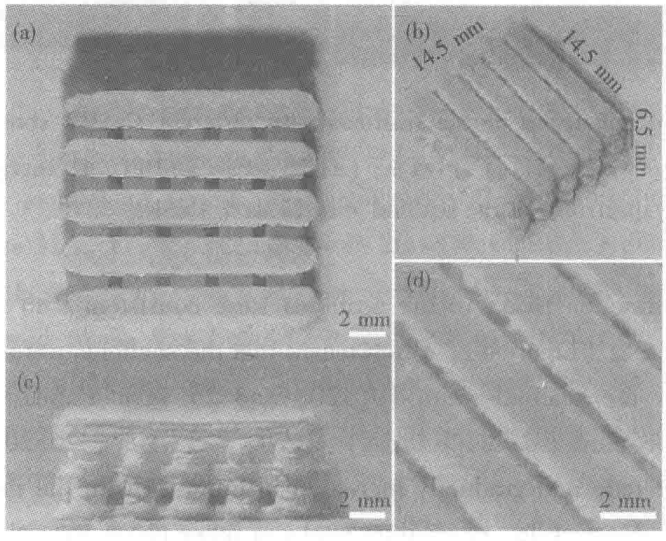

Figure 5 The scaffold with 20 wt% $CaSiO_3$: (a) top view; (b) isometric view; (c) lateral view; and (d) enlarged partial view

3.3 Degradability

Degradability is an important requirement for the bone scaffold to match the process of tissue repair or regeneration[22]. The scaffolds without $CaSiO_3$ hardly degraded; on the contrary, the scaffolds with $CaSiO_3$ continuously degraded after immersion, and the degradation rate increased with the increase of the $CaSiO_3$ (Figure 6). The weight loss percentage of the scaffolds with 20 wt% $CaSiO_3$ was 0.51% on day 7. With the prolonging of the immersion time, it remarkably increased to 3.64% on day 28. As expected, the scaffolds exhibited an improved degradability when $CaSiO_3$ was introduced. The differences of dissolution behavior between Mg_2SiO_4 and $CaSiO_3$ were owing to their difference in chemical composition and crystalline structure[23].

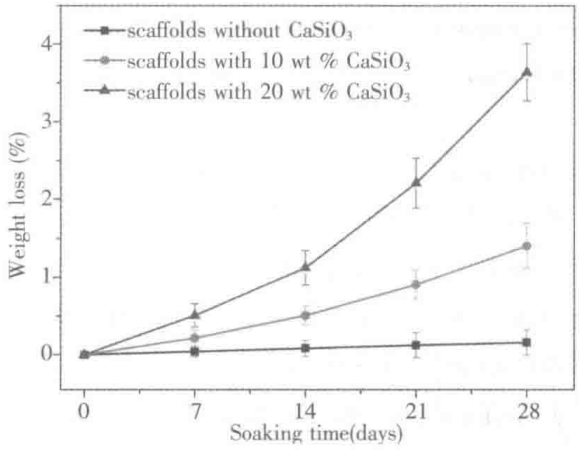

Figure 6 Weight loss of the scaffolds in phosphate buffer saline (PBS) solution

3.4 Bioactivity

The scaffolds without $CaSiO_3$ showed a smooth surface after soaking in SBF for 14 days (Figure 7a), which meant that the Mg_2SiO_4 was short of apatite formability. For the scaffolds with 10 wt% $CaSiO_3$ (Figure 7b), some worm-like particles appeared and uniformly distributed on the scaffolds' surface after 14 days of soaking. With the $CaSiO_3$ increasing to 20 wt% (Figure 7c), the scaffold surface was covered by a dense layer of cauliflower-like precipitates. Furthermore, the elements Ca and P, the main constituent elements of apatite, were detected from an energy dispersive spectroscopy analysis of the cauliflower-like precipitates, which indicated that these precipitates were the bone-like apatite.